smart cities

MDPI

Article

Co-Optimized Scheduling of a Multi-Microgrid System Based on a Reputation Point Trading Mechanism

Jiankai Fang [1,2], Dongmei Yan [1,2,*,†], Hongkun Wang [1,2,*,†], Hui Deng [3], Xinyu Meng [1,2] and Hong Zhang [4,5]

[1] College of Mechanical and Electrical Engineering, Shihezi University, Shihezi 832003, China; jiankaifang@163.com (J.F.)
[2] Corps Key Laboratory of Modern Agricultural Machinery, Shihezi University, Shihezi 832003, China
[3] Zhongxinjian Electric Power Group Co., Ltd., Shihezi 832000, China
[4] College of Energy and Materials, Shihezi University, Shihezi 832003, China
[5] State Key Laboratory of Power System Operation and Control, Tsinghua University, Beijing 100084, China
* Correspondence: 20222109007@stu.shzu.edu.cn (D.Y.); whkmyr@163.com (H.W.)
† These authors contributed equally to this work.

Highlights

What are the main findings?

- A multi-dimensional evaluation framework (incorporating RMSE, MAE, and Dynamic Time Warping) successfully identifies and penalizes fraudulent data or contractual breaches in decentralized energy markets.
- The proposed co-optimized scheduling model achieves a significant reduction in total carbon emissions (49.6 tons) while simultaneously increasing revenues for all participants by 4.08% to 33.00%.

What are the implications of the main findings?

- Coupling social reputation with physical scheduling provides a robust governance structure for Smart Cities to mitigate "trust-risks" and ensure reliability in peer-to-peer trading.
- The synergy between reputation-weighted carbon pricing and demand response demonstrates that environmental decarbonization and economic profitability can be optimized concurrently in multi-microgrid systems.

Abstract

With the rapid integration of distributed energy resources, achieving a balance between economic efficiency and environmental sustainability in multi-microgrid (MMG) systems is critical. However, existing studies typically treat microgrid operators as fully compliant entities. They often neglect the "trust-risk" dimension along with potential default behaviors in decentralized markets. This paper proposes a novel co-optimized scheduling model for urban MMG systems, centered on a unified "Social–Economic–Physical" coupling framework. To ensure transaction integrity, a robust reputation evaluation framework is developed using Root Mean Square Error (RMSE), mean absolute error (MAE), plus Dynamic Time Warping (DTW). This framework effectively identifies fraudulent data or contractual breaches. Furthermore, to enhance fairness while promoting decarbonization, the model integrates a dynamic network pricing strategy based on the Shapley value. It works alongside a reputation-weighted reward–penalty step-type carbon trading scheme. The proposed model is formulated as a mixed-integer linear programming (MILP) problem and solved using MATLAB R2025b with CPLEX 12.10. Simulation results demonstrate that the integrated approach significantly optimizes system performance. Total carbon emissions are reduced by 49.6 tons. Meanwhile, revenues for the MMG Alliance, individual microgrids, and shared energy storage operators increase by 4.08% to 33.00%. The proposed framework provides a practical governance solution for Smart City multi-microgrid

Check for updates

Academic Editor: Pierluigi Siano

Received: 4 February 2026
Revised: 25 March 2026
Accepted: 13 April 2026
Published: 15 April 2026

Copyright: © 2026 by the authors. Licensee MDPI, Basel, Switzerland. This article is an open access article distributed under the terms and conditions of the Creative Commons Attribution (CC BY) license.

systems, effectively addressing the "trust-risk" challenge in decentralized urban energy markets. The findings validate that the proposed mechanism effectively fosters a trustworthy trading environment, achieving a "win-win" outcome for economic profitability and urban energy resilience.

Keywords: multi-microgrid; optimal scheduling; Stackelberg game; trading mechanism

1. Introduction

Smart Cities represent a new paradigm for urban energy governance, where the deep integration of distributed energy resources, 5G real-time communication, and intelligent transaction mechanisms is essential for ensuring resilience and sustainability [1]. Within this context, the secure and reliable operation of smart grid infrastructure has become a foundational requirement. Existing studies highlight that smart grids in urban environments face escalating security challenges—including erroneous data injection, fraudulent transactions, and contractual breaches—that directly undermine the integrity of energy trading and threaten the interests of all participants [2]. Such systemic vulnerabilities demand attention at both the governance and operational levels of Smart City energy infrastructure.

With the increasing penetration of new energy and the development of multi-microgrids (MMGs), the energy market presents characteristics of decentralization and diversification [3]. The interests within MMGs are complex. This necessitates a reasonable trading mechanism to facilitate energy trading among different entities [4]. This mechanism should protect the interests of participants as well as those of the Alliance. Simultaneously, it must curb improper trading behavior of microgrids (MGs) [5,6]. Researchers have examined the advantages versus disadvantages of existing tradable energy market mechanisms, subsequently proposing solutions to current challenges [7]. Others have introduced new trading mechanisms incorporating distributed resources [8]. Some have also developed energy trading models using multi-agent technology with prioritization factors for energy allocation [9].

Reputation-based trading mechanisms have been widely explored, where agents determine reputation values to coordinate trading orders [10]. Some approaches include evaluating reputation based on transaction deviation and rate [11]; quantifying familiarity, acceptance, plus historical performance of MGs [12]; or designing reputation systems for vehicle-to-vehicle transactions based on completion rates [13]. Multi-dimensional reputation models incorporate transaction amount, delivery time, plus feedback mechanisms [9], while others integrate reputation-based matching with electrical distance constraints [14]. The simulation results indicate that these methods effectively incentivize participants to maintain trading discipline [15]. Additionally, distributed trading frameworks that combine coalition chains with multi-agent structures enhance system extensibility.

Carbon trading mechanisms are also important. Dynamic carbon pricing models consider demand response, reducing both operational costs and emissions [16]. Other studies have optimized scheduling by minimizing carbon trading costs [17], or alternatively, proposed step-type carbon pricing mechanisms for near-zero-carbon dispatch [18]. However, existing studies often focus only on regulating MG behavior or reducing their emissions. Given the complexity of energy types coupled with high carbon emissions in MMGs, trading mechanisms must incorporate fraud prevention, default management, plus emission constraints to ensure completeness [19]. Recent work has further extended these mechanisms to coupled multi-microgrid systems incorporating carbon emission trading constraints [20] and peer-to-peer electricity–carbon coupled distribution networks with

dynamic network charges [21], demonstrating the broad technical feasibility of such integrated approaches at the urban scale. Furthermore, recent studies on energy-transfer control that shape the effective charging load profile [22], or those focusing on multi-objective scheduling in water–energy nexus integrated energy systems [23], have a direct impact on the assumed MMG scheduling outcomes.

Frequent transactions risk causing line congestion, thereby increasing MMG maintenance costs. Network tariffs can mitigate this by charging transaction-completed MGs and recovering grid investment costs while influencing market activity [24]. Network tariff mechanisms are classified into two categories: fixed and dynamic. Fixed tariffs are predetermined based on voltage levels, transmission range [14], or electrical distance and grid assets [25], whereas dynamic tariffs are adjusted with real-time network usage [11]. Dynamic approaches include incorporating operation and maintenance costs into market clearing [14], peer-to-peer adjustments considering voltage, line occupancy, and losses [26] or voltage stability and congestion management [25]. Distributed generation planning also informs dynamic tariff models that guide efficient network use. Current research primarily focuses on distribution networks; however, MMG expansion necessitates new tariff mechanisms that account for transaction-induced line impacts [27].

1.1. Research Gap and Motivation

Despite the extensive research on MMG scheduling, there remains a critical research gap in addressing the "trust-risk" dimension within the urban energy context. Existing studies typically treat MGOs as fully rational and compliant entities, neglecting the potential for default behaviors or malicious data falsification in a decentralized market [19]. In a decentralized multi-microgrid energy trading market, "Trust-Risk" is formally defined as the probability and subsequent negative impact of self-interested participants forging forecast data or unilaterally refusing physical fulfillment due to the lack of absolute centralized regulation, which ultimately leads to energy supply–demand imbalances across the entire network and unfair acquisition of improper benefits. Furthermore, current carbon trading and network pricing models are often decoupled from the credit status of participants, leading to the "tragedy of the commons" where non-compliant actors exploit the system without penalty. In the context of Smart Cities, where energy resilience and data integrity are paramount, a unified framework that couples social credit (reputation), economic incentives (pricing), and physical constraints (carbon/grid) is urgently needed.

1.2. Contributions

To address these challenges, this study proposes a reputation-based co-optimized scheduling mechanism for urban MMG systems. The main contributions are:

1. A multi-dimensional Reputation Evaluation Mechanism is established to quantify transaction compliance, directly linking MGOs' trustworthiness to their market trading priority plus penalty weights.
2. A dynamic network pricing strategy based on the Shapley value is integrated to ensure fair cost allocation while coupling network constraints with economic incentives.
3. A bi-level low-carbon scheduling model is formulated for Smart City multi-microgrid systems, fully coupling the multi-dimensional constraints of reputation points, economic incentives, as well as physical operations (Credit-Economic-Physical) to achieve a "win-win" for economic efficiency alongside urban decarbonization and energy resilience.

2. System Framework and Trading Mechanism

Within the distributed interaction framework, the microgrid operator (MGO) performs real-time information transmission and energy interaction with the Alliance. Simultaneously, it maintains the internal Gas Turbines (GTs) and Gas Boilers (GBs) through unidirectional interaction with the natural gas grid. As they lack individual energy storage devices, MGOs can only store electrical and thermal energy through shared storage and transmit real-time information via the 5G network. The energy interactions among the MGO are shown in Figure 1. MGOs are the primary participants in energy trading. They have the capacity to propose energy prices autonomously and transmit their information to the Alliance, which disseminates this information on their behalf. The Alliance is responsible for coordinating energy transactions within the MMG [7] and providing auxiliary functions. In instances where the internal MMG transaction is unable to satisfy demand or is precluded from participation, the MGO engages in trade activities with the higher-level energy network through the Alliance.

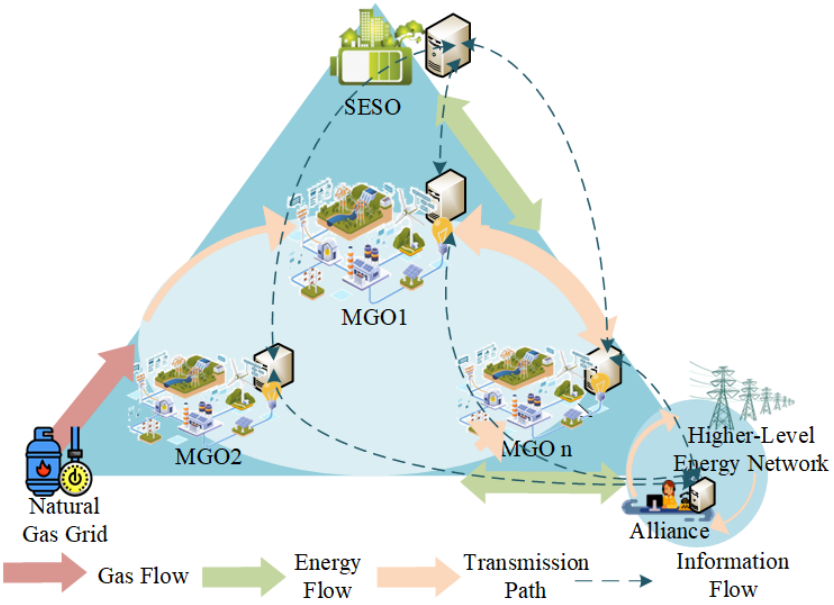


Figure 1. The distributed MMG system subject interaction relationships.

2.1. Subject of the Trading Mechanism

In the MMG, energy trading is facilitated through a reputation point trading mechanism, with multiple subjects participating in this process. The specific forms of energy traded include electricity and thermal energy. The following subjects are primarily involved in this trading.

2.1.1. Alliance

The Alliance functions both as a market subject and a user. It engages in two-way energy transactions with MGOs and higher-level energy networks while maintaining market order and evaluating member reputation.

2.1.2. MGO

The MGO operates on a model of self-generation and self-consumption, selling surplus energy to meet its needs.

2.1.3. Higher-Level Energy Network

Engages in energy trading with the Alliance as a market subject.

2.1.4. Shared Energy Storage Operator (SESO)

Offers leasing services for electric and thermal energy storage, flexibly allocating storage based on market demand [14,25].

2.2. Rule on Trading Mechanism

2.2.1. Reputation Judgment

The MGO facilitates the provision of anonymized load and distributed energy forecast data, as well as real-time data prior to the transaction. The Alliance then archives and analyses the data submitted by the current MGO. It employs a set of three indexes: root mean square deviation, mean absolute error, and similarity. These indexes evaluate performance and ascertain the presence of any fraudulent activity [28]. Subsequent to the transaction's conclusion, the Alliance is responsible for ascertaining whether the MGO has fulfilled its energy delivery obligations in a timely manner. It also verifies whether there has been any contravention of the contractual agreement. Comparing the values of the MGO submission data with the Alliance forecast data and the MGO historical day similar data, the following indices were obtained:

- RMSE and MAE are used to evaluate deviations between MGO submitted data and both Alliance predictions and historical similar data. To eliminate the dimensional impacts of different microgrid installed capacities, Min-Max scaling is applied to normalize the input data before calculating the indices. The formulas are as follows:

$$I_{\mathrm{RMSE}} = \sqrt{\frac{1}{T}\sum_{t=1}^{T}(P_n^{sub}(t) - P_n^{ref}(t))^2} \tag{1}$$

$$I_{\mathrm{MAE}} = \frac{1}{T}\sum_{t=1}^{T}|P_n^{sub}(t) - P_n^{ref}(t)| \tag{2}$$

  where $P_n^{sub}(t)$ and $P_n^{ref}(t)$ denote the normalized submitted data and reference data at time t, respectively.
- DTW calculates sequence similarity. It effectively handles unequal-length alignment and matching issues owing to data loss. The normalized path cumulative distance is expressed as:

$$I_{\mathrm{DTW}} = 1 - \frac{D_{DTW}(P_n^{sub}, P_n^{ref})}{D_{max}} \tag{3}$$

  where D_{DTW} is the cumulative distance of the optimal warping path, and D_{max} is the maximum possible discrete distance used for normalization.
- The installation of smart meters is undertaken at the exit of the MGO connection line. The smart meter is in a state of uninterrupted recording and stores the monitoring information. In the event of a transaction at the MGO, the Alliance can obtain real-time energy interaction information detected by the smart meter. This information is then used to determine whether there has been a breach of contract at an MGO. To maintain the privacy of MGO data, the Alliance only obtains the relevant monitoring information for verification when a transaction is in progress [9].

Due to the different characteristics of various new energy outputs, their evaluation indexes are slightly different, in which the PV index should meet $I_{\mathrm{RMSE}} < 1.6$, $I_{\mathrm{MAE}} < 0.7$, $I_{\mathrm{DTW}} > 85\%$; the WT index should meet $I_{\mathrm{RMSE}} < 2$, $I_{\mathrm{MAE}} < 1.5$, and $I_{\mathrm{DTW}} > 85\%$ [25]. It should be noted that the 85% threshold (and other specific thresholds) is not a strict mathematical derivation but an empirical parameter. It is established by simulating a full year of

historical operating data and extracting the 95% confidence interval of the error distribution. Further sensitivity analysis of these thresholds will be discussed in subsequent sections.

2.2.2. Point Mechanism

The reputation of the MGO is incorporated into the energy trading mechanism to regulate trading behavior, with an initial score of 3 points and a trading cycle of 7 days. The exact daily update, award, and penalty rules are explicitly listed as follows:

- **Initial Score:** Each MGO starts with an initial reputation score of 3 points.
- **Penalty for Minor Default / Breach:** If an MGO fails to conduct transactions in accordance with the contract content, its reputation points will be reduced by 1 point. The MGO is prohibited from participating in the internal energy transactions of the MMG system on the same day.
- **Penalty for Severe Fraud:** If the Alliance determines, through data judgment, that an MGO has committed severe data fraud, its reputation points will be heavily penalized by 2 points.
- **Suspension Rule:** When the reputation points are less than 1, the MGO is prohibited from participating in all internal transactions within the current trading cycle.
- **Reward for Low-Carbon Operation:** Considering the carbon emission issue, I_{h} is proposed to advocate low-carbon operation. Following the conclusion of a scheduling cycle, the MGO with the most significant I_{h} (and no violations) is awarded 1 reputation point, where

$$\mathrm{I}_{h} = \frac{\mathrm{F}_{\mathrm{n,C}}^{\mathrm{d}} - \mathrm{F}_{\mathrm{n,C}}^{\mathrm{d}-1}}{\mathrm{F}_{\mathrm{n,C}}^{\mathrm{d}-1}} \times 100\% \tag{4}$$

  $\mathrm{F}_{\mathrm{n,c}}^{\mathrm{d}}$ denotes the carbon transaction cost of the $\mathrm{MGO_n}$ in the d th scheduling cycle, while $\mathrm{F}_{\mathrm{n,c}}^{\mathrm{d}-1}$ represents the carbon transaction cost of the $\mathrm{MGO_n}$ in the $d-1$ scheduling cycle. Furthermore, to ensure market **Fairness**, a parallel reward rule is introduced: *if a given MGO's clean energy ratio consistently reaches* 95% *or above and it demonstrates no violation behaviors for three consecutive scheduling cycles, it is also rewarded 1 point*. This addresses the unfair penalty toward clean microgrids lacking additional emission reduction potential.
- **Penalty Pricing:** In the event of fraudulent or defaulting MGO behavior, energy is purchased at $(1+\gamma)$ times the price from the subsequent day. At this point, the energy seller receives revenue at the original price, and the Alliance receives the remaining revenue [8].

$$\gamma = \gamma_{\mathrm{bas}} + (\beta - 1)\tau \tag{5}$$

  where the base penalty factor is denoted by γ_{bas}, the current number of frauds and defaults by β, and the penalty factor growth rate by τ. In instances where the $(1+\gamma)$ times price is higher than the price of energy from the higher-level energy network, the MGO purchases energy in accordance with the price of the higher-level energy network.
- **Transaction Negotiation:** In the context of the transaction, MGOs are required to submit energy transaction information on an hourly basis. In response, the Alliance disseminates real-time energy price information. Subsequently, MGOs are expected to respond to the Alliance by submitting their energy purchase and sale strategies on an hourly basis [29]. The dynamic interaction between the MGOs is characterized by a process of negotiation, whereby the parties reach a mutually beneficial agreement when it becomes evident that altering the price strategy alone will not yield improvements to their respective interests.

The MGO participating in the transaction submits energy transaction information on an hourly basis; subsequently, the Alliance releases real-time energy price information. In response, the MGO submits energy purchase plus sale strategies hourly. The game is played between MGOs; eventually, the subjects reach a deal when they cannot improve their own interests by changing their price strategies alone. When there is competition among MGOs of the same kind, under the coordination of the Alliance, the MGO with the larger demand in the previous scheduling cycle has priority in meeting the energy demand. When all transactions are completed, if there are still MGOs that have not met the demand, they will conduct transactions with the higher-level energy network through the Alliance.

2.3. Dynamic Network Tariff Trading Mechanism Based on Shapley Value

The Shapley value is a prevalent economic methodology for benefit distribution and cost-sharing. It can be used to calculate the marginal contribution of each participating subject to cooperation, thereby determining the reasonable share of each subject in the total cost [5]. The mechanism determines the marginal contribution of the MGO's trading volume to the total number of transactions in the MMG system based on the Shapley value and apportions the network tariffs to the MGO. To avoid double counting the transaction volume, the transaction volume of the energy-purchasing MGOs is used as a baseline in the process of setting the network tariffs.

$$\boldsymbol{\phi}_j(t) = \sum_{j \subset Q, f \subset F_i} \frac{(|f|-1)!(j-|f|)!}{j!} \left[c_f(t) - c_{f/\{j\}}(t) \right] \tag{6}$$

where j is the energy-purchasing $\mathrm{MGO_j}$, $j \in [1, 2, \cdots, j, \cdots, J]$; $\phi_j(t)$ is the marginal trading contribution of the energy-purchasing $\mathrm{MGO_j}$; Q is the set of all MGOs; F is the set formed by all subsets of Q; f is a subset of F; $|f|$ is the number of elements of the set f; $C_f(t)$ denotes the trading volume of all energy-purchasing MGOs participating in the energy trade at t moment; $C_{f/\{j\}}(t)$ is the trading volume of the remaining energy-purchasing MGOs, excluding the purchasing $\mathrm{MGO_j}$, when they participate in the energy trade at t moment. In this study, the network tariff is principally derived from connection line construction and operation and maintenance costs [24].

$$C_{\mathrm{anv}} = \frac{(1+\alpha)}{365} \sum_{l=1}^{L} C_{\mathrm{load}} X_l \frac{r(1+r)^Y}{(1+r)^Y - 1} \tag{7}$$

$$\omega_{\mathrm{t}-j}(t) = \frac{C_{\mathrm{anv}} \phi_j(t)}{T \sum_{j=1}^{J} \phi_j(t)} \tag{8}$$

where C_{anv} is the average daily cost of construction and operation and maintenance of the Alliance lines; α is the annual discount factor for the cost of operation and maintenance of the Alliance lines; l denotes the lth line; L is the total number of lines constructed by the Alliance; C_{load} is the construction cost per unit length of a line; X_l is the length of the lth line; r is the discount rate of the line; and Y is the useful life of the line; and $\omega_{t-j}(t)$ is the network tariff incurred by energy purchase $\mathrm{MGO_j}$ at t moment.

$$\omega_{\mathrm{n}}(\mathrm{t}) = \begin{cases} \omega_{\mathrm{t-j}}(\mathrm{t})/2 & \mu_{\mathrm{MMG,n}}(\mathrm{t}) = 1 \\ \omega_{\mathrm{t-j}}(\mathrm{t}) & \mu_{\mathrm{MMG,n}}(\mathrm{t}) = 0 \text{ and } \mu_{\mathrm{g,n}}(\mathrm{t}) = 1 \\ 0 & \mu_{\mathrm{MMG,n}}(\mathrm{t}) = 0 \text{ and} \mu_{\mathrm{g,n}}(\mathrm{t}) = 0 \end{cases} \tag{9}$$

where $\omega_n(t)$ denotes the network tariff that is to be paid by the MGO_n, $\mu_{MMG,n}(t)$ is the transaction variable of the MGO_n, which trades with other MGO_s when $\mu_{MMG,n}(t) = 1$ and trades with the Alliance when $\mu_{MMG,n}(t) = 0$.

$\mu_{g,n}(t)$ is the state variable of the MGO_n, which is in the state of purchasing energy when $\mu_{g,n}(t) = 1$ and in the state of selling energy when $\mu_{g,n}(t) = 0$. When MGO_n trades with other MGOs, $\mu_{MMG,n} = 1$, both of the MGOs share the network tariff; when MGO_n purchases energy from the Alliance, $\mu_{MMG,n} = 0$ and $\mu_{g,n}(t) = 1$, the MGO_n bear the network tariff individually; and when MGO_n sell energy to the Alliance, $\mu_{MMG,n} = 0$ and $\mu_{g,n}(t) = 0$, the MGO_n do not have to pay the network tariff.

2.4. Transaction Mechanism Process

The reputation-point transaction mechanism mainly includes four transaction links.

2.4.1. Demand Submission and Reputation Judgment

The MGO's intelligent decision system autonomously generates trading demands based on real-time load, generation forecasts, and pricing data. The Alliance accounting system performs an initial screening, rejecting submissions from operators with reputation scores below 1. Validated requests undergo fraud detection before proceeding to the Alliance system [15].

2.4.2. Demand Confirmation and Announcement

The Alliance system verifies feasibility and prioritizes transactions using a reputation-based ranking mechanism. Matched transactions are processed automatically, whereas unmatched demands are published for potential matches with higher-tier operators or shared storage providers (SESOs).

2.4.3. Transaction Execution and Verification

Matched transactions are executed via MGO smart terminals with real-time monitoring of the load, generation, and power flows. Smart contracts automate settlements [12], whereas the Alliance system validates compliance using smart meter data.

2.4.4. Network Tariff Accounting and Reputation Announcement

Following transaction completion, the Alliance's intelligent system calculates and collects network tariffs from participating MGO_n using (6)–(8), with detailed billing statements that are available for audit. At the conclusion of the daily cycle (24:00), the system computes updated reputation scores via (4) and disseminates the revised rankings to all MMG participants [15].

The following steps are observed by the MGO when conducting transactions:

- **Step 1:** The Alliance determines whether the MGO is permitted to participate in the transaction based on its reputation point.
- **Step 2:** The MGO with reputation points > 1 submit time-of-use energy price information, load and other relevant data.
- **Step 3:** The Alliance determines whether the MGO has engaged in fraudulent behavior. If it has, the MGO is prohibited from participating in the same-day energy transaction with a deduction of 1reputation point. The Alliance disseminates time-of-use energy pricing information.
- **Step 4:** The MMG trades internally and feeds back the trading results to the Alliance.
- **Step 5:** The Alliance determines whether the MGO has traded in accordance with the contract content based on the MGO's feedback information and the contract line smart meter. MGOs with defaults have a deduction of 1reputation point.

- **Step 6:** The Alliance accounts for the network tariff.
- **Step 7:** At the end of a dispatch cycle, the MGO with the largest I_h receives 1 reputation point.
- **Step 8:** The transaction ends.

3. The Low-Carbon Scheduling Model Under the Reputation-Point Trading Mechanism

The bi-level optimization framework establishes an economic low-carbon operation mechanism for multi-microgrid systems using a step-type carbon trading model with reward–punishment characteristics [16,30]. As illustrated in Figure 2, the upper-level Alliance operates as the leader, determining and broadcasting time-of-use energy pricing information to participating microgrid operators [24]. At the lower level, microgrid operators function as followers that autonomously develop operational strategies to maximize their individual revenues. These strategies incorporate local renewable energy generation profiles, load demand patterns, and pricing information from peer operators [31]. The formulated strategies undergo iterative refinement through continuous feedback between both levels until reaching an equilibrium state, where no participant can improve their position through unilateral changes.

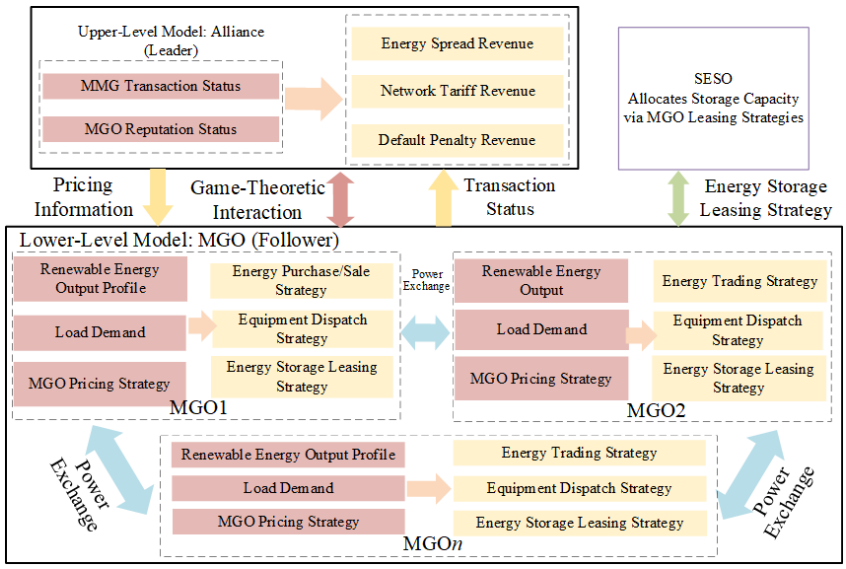


Figure 2. MMG bi-level optimal scheduling model framework.

3.1. Social–Economic–Physical Coupling Framework

The core of this model is the unified "Social–Economic–Physical" coupling framework. Mathematically, the **Social** dimension is represented by a binary reputation state variable $\mu_n \in \{0, 1\}$, which quantifies the trustworthiness of MGO_n. Economically, a poor reputation ($\mu_n = 0$) acts as a multiplier cutting off regular peer-to-peer trading paths ($\mu_n F_{n,\mathrm{micro}}$), forcing the MGO to trade exclusively with the Alliance under an altered penalty pricing factor γ (**Economic** dimension). Physically, these socio-economic constraints strictly bound the underlying power flow limits and carbon emission outputs (**Physical** dimension), achieving rigorous mathematical synergy across all three domains.

3.2. Optimization Objective

3.2.1. The Upper-Level Model

The upper-level model is designed to optimize the maximum Alliance revenue. This revenue is primarily derived from three sources, energy spread revenue, network tariff revenue, and default penalty revenue, which are expressed as follows:

$$F_{n,\text{sell}}^{\text{micro}} = \sum_{t=1}^{T}((\lambda_{\text{s}}(t) - \lambda_{\text{p}}(t))P_{n,\text{sell}}^{\text{micro}}(t) + (\lambda_{\text{h,s}}(t) - \lambda_{\text{h,p}}(t))P_{n,\text{h,sell}}^{\text{micro}}(t)) \tag{10}$$

- **Energy spread revenue** $F_{n,\text{sell}}^{\text{micro}}$**:** In instances where the MGO experiences an excess of energy or is unable to trade with other MGOs due to circumstances such as fraud, the Alliance can purchase energy from the MGO. It subsequently sells this energy to other MGOs at the higher-level energy network time-of-use energy price. This process generates revenue for the Alliance. If the energy sold by the Alliance to the MGO originates from a higher-level energy network, the Alliance does not receive revenue, as there is no price difference. Here, $\lambda_{\text{s}}(t)$ and $\lambda_{\text{p}}(t)$ represent the unit selling and purchasing electricity prices of the higher-level energy network at time t, respectively; $\lambda_{\text{h,s}}(t)$ and $\lambda_{\text{h,p}}(t)$ denote the unit selling and purchasing thermal prices of the higher-level energy network at time t, respectively; $P_{n,\text{sell}}^{\text{micro}}(t)$ and $P_{n,\text{h,sell}}^{\text{micro}}(t)$ represent the electrical and thermal energy spread that the Alliance sells to other MGOs from MGO_n at time t to act as a mid-broker, respectively; and T is the number of total periods in the dispatch cycle.
- **Network tariff revenue** $F_{n,\omega}$**:**

$$\text{F}_{\text{n,!}} = \sum_{\text{t=1}}^{\text{T}} !_{\text{n}}(\text{t}) \tag{11}$$

- **Default penalty revenue** $F_{n,\gamma}^{\text{micro}}$**:** When the MGO_n is fraudulent and trades energy with the Alliance during the trading cycle, it pays no additional penalty fee. This is because the Alliance trades at the higher-level energy network price. However, when the MGO_n is fraudulent and purchases energy from other MGOs during the trading cycle, the Alliance generates the penalty benefit as follows:
  When the MGO_n engages in fraudulent trading, the Alliance's penalty revenue is calculated as follows:

$$F_{n,C} = \sum_{i=1}^{\tau}\begin{cases} -c(E_{n,0}(t) - E_n(t)) & E_n(t) \le E_{n,0}(t) \\ c(E_n(t) - E_{n,0}(t)) & E_{n,0}(t) < E_n(t) \le E_{n,0}(t) + \omega \\ c\omega + c(1+\nu)(E_n(t) - E_{n,0}(t) - \omega) & E_{n,0}(t) + \omega < E_n(t) \le E_{n,0}(t) + 2\omega \\ c\omega + c(1+2\nu)(E_n(t) - E_{n,0}(t) - 2\omega) & E_{n,0}(t) + 2\omega < E_n(t) \le E_{n,0}(t) + 3\omega \\ c\omega + c(1+3\nu)(E_n(t) - E_{n,0}(t) - 3\omega) & E_{n,0}(t) + 3\omega < E_n(t) \end{cases} \tag{12}$$

3.2.2. The Lower-Level Model

In the lower-level model, the MGO receives the price information released by the Alliance and takes the maximum of its own revenue as the optimization objective [8]. The total revenue of the MGO n is formulated as:

$$\max F_{MGO,n} = F_{n,load} + F_{n,micro} - F_{n,grid} - F_{n,gas} - F_{n,C} - F_{n,share} \tag{13}$$

where μ_n denotes the reputation state variable. If $\mu_n = 0$, the MGO is prohibited from internal trading.

The reputation state variable of MGO^n is denoted by μ_n. In the event of $\mu_n = 0$, the MGO^n has fraudulent behavior during the current trading day and is prohibited from participating in the MMG trading and can only trade with the Alliance according to the higher-level energy network price. Conversely, when $\mu_n = 1$, the MGO^n engages in trading in the conventional manner.

- **Revenue from selling energy to users** $F_{n,load}$**:**

$$F_{n,\text{load}} = \sum_{t=1}^{T} (\lambda_{\text{s}}(t) P_{n,\text{load}}(t) + \lambda_{\text{h,s}}(t) P_{n,\text{h,load}}(t)) \tag{14}$$

The MGO sells energy to internal users at a time-of-use energy price from the higher-level energy network, where the electrical and thermal loads are within the MGO, respectively.

To mobilize users to participate in the system energy scheduling, an electric load demand response model considering real-time price and thermal load demand response model considering comfort level are developed [29]:

$$\mathbf{P}_{n,\text{load}} = \mathbf{P}^0_{n,\text{load}} + \boldsymbol{E} \cdot \frac{\Delta \mathbf{s}}{\mathbf{s}} \tag{15}$$

where the vectors are expressed over time as $\mathbf{P}_{n,\text{load}} = [P_{n,\text{load}}(1), \ldots, P_{n,\text{load}}(T)]^\top$, representing the optimized electrical load; $\mathbf{P}^0_{n,\text{load}} = [P^0_{n,\text{load}}(1), \ldots, P^0_{n,\text{load}}(T)]^\top$ represents the initial load profile before demand response; and

$$\frac{\Delta \mathbf{s}}{\mathbf{s}} = [\Delta s(1)/s(1), \ldots, \Delta s(T)/s(T)]^\top$$

denotes the relative price variance. $\boldsymbol{E}$ is the $T \times T$ price response elasticity matrix, where its diagonal element ε_{uv} $(u = v)$ denotes the auto-elasticity coefficient, and $u \neq v$ represents the cross-elasticity coefficient for inter-temporal load shifting $(u, v \in [1, T])$; s_t is the initial real-time price at time t; and $\Delta s(t)$ is the amount of change in price relative to the initial tariff.

$$P_{n,\text{h,load}}(t) = \frac{1}{R}\left(\frac{T^{\text{temp}}_{\text{in}}(t+1) - kT^{\text{temp}}_{\text{in}}(t)}{1-k} - T^{\text{temp}}_{\text{out}}(t)\right) \tag{16}$$

$$k = e^{-\frac{\Delta t}{\tau}} \tag{17}$$

$$\tau = RC_{\text{air}} \tag{18}$$

where R denotes the equivalent thermal resistance of the building; $T^{temp}_{in}(t)$ and $T^{temp}_{out}(t)$ represent the indoor and outdoor environmental temperature at time t, respectively; C_{air} is the indoor thermal capacity; Δt is the discrete scheduling time interval step; the subscript n specifies parameters belonging to the n-th MGO index.

- **MMG trading revenue** $F_{n,micro}$**:**

$$\begin{aligned} F_{n,\text{micro}} = \sum_{t=1}^{T} \sum_{z=1\&z\neq n}^{N} & (s_{n,s}(t) P_{z-n,\text{sell}}(t) + s_{n,\text{h,s}}(t) P_{z-n,\text{h,sell}}(t) \\ & - s_{z,s}(t) P_{z-n,\text{buy}}(t) - s_{z,\text{h,s}}(t) P_{z-n,\text{h,buy}}(t)) \end{aligned} \tag{19}$$

where $S_{n,s}(t)$ and $S_{n,h,s}(t)$ are the time-of-use electricity and thermal price of MGO^n, respectively; and $P_{z-n,sell}(t)$ and $P_{z-n,h,sell}(t)$ are the electricity and thermal energy sold by MGO^n to MGO^z, respectively.

- **Transaction cost with the Alliance** $F_{n,grid}$**:**

$$F_{n,\text{grid}} = \sum_{t=1}^{T}(\lambda_{\text{s}}(t)P_{n,\text{sell}}(t) - \lambda_{\text{p}}(t)P_{n,\text{buy}}(t) + \lambda_{\text{h,s}}(t)P_{n,\text{h,sell}}(t) - \lambda_{\text{h,p}}P_{n,\text{h,buy}}(t)) \tag{20}$$

where $P_{n,sell}(t)$ and $P_{n,h,sell}(t)$ represent the electricity and thermal energy sold by the Alliance to MGO^n, respectively; $P_{n,buy}(t)$ and $P_{n,h,buy}(t)$ represent the electricity and thermal energy purchased by the Alliance from MGO, respectively.

- **Cost of gas purchased** $F_{n,gas}$**:** Carbon emissions from the MGO mainly come from three components: GT, GB and energy purchased by the MGO from the Alliance. Among them, the energy from the MGO sold by the Alliance to MGOs mainly comes from four parts: PV, WT, GT, and GB. PV and WTs are regarded as having no pollutant emissions. In contrast, the pollutants generated by a GT and GB are calculated in the pollutant emission penalty cost of each MGO. Therefore, only the carbon transaction cost of the energy from the higher-level energy network sold by the Alliance to the MGO is calculated. The initial carbon emission quota $E_{n,0}(t)$ and actual carbon emission $E_n(t)$ are

$$E_{n,0}(t) = \sigma_{\text{h}}(P_{n,\text{GT}}(t) + Q_{n,\text{GB}}(t)) + \sigma_{\text{e}}(P^{\text{grid}}_{n,\text{sell}}(t) + P^{\text{grid}}_{n,\text{h,sell}}(t)) \tag{21}$$

$$E_n(t) = E_{n,\text{GT}}(t) + E_{n,\text{GB}}(t) + E^{\text{grid}}_{n,\text{in}}(t) \tag{22}$$

$$\begin{cases} E_{n,GT}(t) = \varepsilon_{\text{h}}P_{n,GT}(t) \\ E_{n,GB}(t) = \varepsilon_{\text{h}}Q_{n,GB}(t) \\ E^{\text{grid}}_{n,\text{in}}(t) = \varepsilon_{\text{e}}\left(P^{\text{grid}}_{n,\text{sell}}(t) + P^{\text{grid}}_{n,\text{h,sell}}(t)\right) \end{cases} \tag{23}$$

where σ_h is the carbon emission quota per unit of thermal supplied by the GT and GB; σ_e is the carbon emission quota per unit of energy supplied by the Alliance; $P_{n,GT}(t)$ and $Q_{n,GB}(t)$ are the output power of the GT and GB from MGO^n at t moment; $\mathbb{E}_{n,GT}(t)$, $\mathbb{E}_{n,GB}(t)$, $E^{\text{grid}}_{n,\text{in}}(t)$ are the actual carbon emissions of the GT, GB, and the Alliance, respectively; ε_{h} is the actual carbon emissions per unit of the GT and GB; ε_{e} is the actual carbon emissions per unit of the Alliance; $P^{\text{grid}}_{n,\text{sell}}(t)andP^{\text{grid}}_{n,\text{h,sell}}(t)$ and are the electrical and thermal energy from the higher-level energy network sold by the Alliance to MGO^n, respectively. If $E_n(t) < E_{n,0}(t)$, the reward is given; if $E_n(t) > E_{n,0}(t)$, $F_{n,c}$ is calculated based on the quantitative relationship between the two [27,32]:

$$F_{n,C} = \sum_{i=1}^{\tau}\begin{cases} -c(E_{n,0}(t) - E_n(t)) & E_n(t) \le E_{n,0}(t) \\ c(E_n(t) - E_{n,0}(t)) & E_{n,0}(t) < E_n(t) \le E_{n,0}(t) + \omega \\ c\omega + c(1+\nu)(E_n(t) - E_{n,0}(t) - \omega) & E_{n,0}(t) + \omega < E_n(t) \le E_{n,0}(t) + 2\omega \\ c\omega + c(1+2\nu)(E_n(t) - E_{n,0}(t) - 2\omega) & E_{n,0}(t) + 2\omega < E_n(t) \le E_{n,0}(t) + 3\omega \\ c\omega + c(1+3\nu)(E_n(t) - E_{n,0}(t) - 3\omega) & E_{n,0}(t) + 3\omega < E_n(t) \end{cases} \tag{24}$$

where c is defined as the price per unit of carbon emission; ω represents the length of the carbon emission interval; and ν is the increase in price per unit of carbon emission interval.

- **Energy storage lease cost** $F_{n,share}$**:**

$$F_{n,\text{share}} = \sum_{t=1}^{T}(\gamma_l(P_{n,\text{dis}}(t) + P_{n,\text{ch}}(t)) + \gamma_h(P_{n,\text{h,dis}}(t) + P_{n,\text{h,ch}}(t))) \quad (25)$$

where γ_l and γ_h are the price per unit of electric and thermal power for leasing the SESO, respectively; $P_{n,\text{dis}}(t)$ and $P_{n,h,\text{dis}}(t)$ denote the electric and thermal energy released by the SESO to MGO^{n}, respectively; $P_{n,\text{ch}}(t)$ and $P_{n,h,\text{ch}}(t)$ denote the electric and thermal energy stored by MGO^{n} to the SESO, respectively.

3.2.3. Shared Energy Storage Revenue

SESO receives revenue by providing energy storage leasing services to the MGO, the cost of which consists mainly of the operating cost of the energy storage devices, and the revenue function $F_{\mathbf{s}}$ is as follows [14,33,34]:

$$F_{\text{s}} = \sum_{n=1}^{N}(F_{n,\text{share}} - F_{n,\text{ce}}) \quad (26)$$

$$F_{n,\text{ce}} = \sum_{t=1}^{T}(\varepsilon^{\text{ch}}P_{n,\text{ch}}(t)\Delta t + \varepsilon^{\text{dis}}P_{n,\text{dis}}(t)\Delta t + \varepsilon_{\text{h}}^{\text{ch}}P_{n,\text{h,ch}}(t)\Delta t + \varepsilon_{\text{h}}^{\text{dis}}P_{n,\text{h,dis}}(t)\Delta t) \quad (27)$$

where A is the operating cost of the energy storage device; $\varepsilon^{\mathbf{ch}}$ and $\varepsilon^{\mathbf{dis}}$ are the unit charging and discharging operating costs of electric energy storage, respectively; $\varepsilon_{\text{h}}^{\mathbf{ch}}$ and $\varepsilon_{\text{h}}^{\mathbf{dis}}$ are the unit charging and discharging operating costs of thermal energy storage, respectively.

3.3. Constraint

To guarantee the secure operation of the system, the output of each piece of equipment must satisfy the power constraints that are present during actual operation, and the interaction power of each contact line must satisfy the power constraints in the actual operational context. Furthermore, the following equation must be satisfied.

3.3.1. Price Constraint

To attract other MGOs to engage in trade, the time-of-use energy price of MGO^{n} must satisfy the following condition: it should not be higher than the selling price of the higher-level energy network, and it should not be lower than the purchase price [8]:

$$\lambda_{\text{p}}(t) \le s_{n,\text{s}}(t) \le \lambda_{\text{s}}(t) \quad (28)$$

$$\lambda_{\text{h,p}}(t) \le s_{n,\text{h,s}}(t) \le \lambda_{\text{h,s}}(t) \quad (29)$$

3.3.2. Load Demand Response Constraint

The following constraints should be satisfied to prevent over-responses from affecting the normal operation of the system and reducing user comfort [29]:

$$-\Delta P_{n,\text{load}}^{\text{lat,max}}(t) \le \Delta P_{n,\text{load}}^{\text{lat}}(t) \le \Delta P_{n,\text{load}}^{\text{lat,max}}(t) \quad (30)$$

$$\text{T}_{\text{min}}^{\text{temp}}(\text{t}) \le \text{T}_{\text{in}}^{\text{temp}}(\text{t}) \le \text{T}_{\text{max}}^{\text{temp}}(\text{t}) \quad (31)$$

where $\Delta\text{P}_{n,load}^{lat,max}(t)$ is the maximum change in electrical load, $\text{T}_{\text{min}}^{temp}(t)$ and $\text{T}_{\text{max}}^{temp}(t)$ are the minimum and maximum values of indoor temperature change.

3.3.3. Power Balance Constraints

The following power balance constraint should be satisfied to guarantee the proper operation of MGO^{n}:

$$\begin{aligned} P_{n,\mathrm{load}}(t) + P_{n,\mathrm{buy}}(t) + P_{n,\mathrm{ch}}(t) + P_{z-n,\mathrm{sell}}(t) = & P_{n,\mathrm{sell}}(t) + P_{n,\mathrm{GT}}(t) + P_{n,\mathrm{dis}}(t) \\ & + P_{n,\mathrm{PV}}(t) + P_{z-n,\mathrm{buy}}(t) + P_{n,\mathrm{WT}}(t) \end{aligned} \tag{32}$$

$$\begin{aligned} P_{n,\mathrm{hload}}(t) + P_{n,\mathrm{h,buy}}(t) + P_{n,\mathrm{h,ch}}(t) + P_{z-n,\mathrm{h,sell}}(t) = & P_{n,\mathrm{h,sell}}(t) + Q_{n,\mathrm{GB}}(t) + Q_{n,\mathrm{GT}}(t) \\ & + P_{n,\mathrm{h,dis}}(t) + P_{z-n,\mathrm{h,buy}}(t) \end{aligned} \tag{33}$$

where $P_{n,\mathrm{PV}}(t)$ and $P_{n,\mathrm{WT}}(t)$ are the output power of the Photovoltaic (PV) and Wind Turbine (WT) units of MGO$_n$, respectively.

3.3.4. Equipment Operation Constraints

To ensure the logical operation of the physical equipment within the microgrid, the output of controllable distributed generation units (Gas Turbines and Gas Boilers) must be constrained by their capacity limits and ramp rates:

$$P_{n,GT}^{min} \le P_{n,GT}(t) \le P_{n,GT}^{max} \tag{34}$$

$$Q_{n,GB}^{min} \le Q_{n,GB}(t) \le Q_{n,GB}^{max} \tag{35}$$

$$\begin{cases} -R_{n,GT}^{down} \le P_{n,GT}(t) - P_{n,GT}(t-1) \le R_{n,GT}^{up} \\ -R_{n,GB}^{down} \le Q_{n,GB}(t) - Q_{n,GB}(t-1) \le R_{n,GB}^{up} \end{cases} \tag{36}$$

where $P_{n,GT}^{max}/P_{n,GT}^{min}$ and $Q_{n,GB}^{max}/Q_{n,GB}^{min}$ represent the upper and lower output limits; R^{up} and R^{down} denote the ramp-up and ramp-down rates, respectively.

3.3.5. Shared Energy Storage Constraints

The operation of the Shared Energy Storage Operator (SESO) must satisfy the state-of-charge (SOC) continuity and capacity limits. To prevent simultaneous charging and discharging, a Boolean variable logic is applied (simplified here for linear formulation):

$$S(t) = S(t-1) + \sum_{n=1}^{N} \left(P_{n,ch}(t)\eta_{ch} - \frac{P_{n,dis}(t)}{\eta_{dis}} \right) \Delta t \tag{37}$$

$$E_{bat}^{min} \le S(t) \le E_{bat}^{max} \tag{38}$$

$$S(T) = S(0) \tag{39}$$

$$0 \le \sum_{n=1}^{N} P_{n,ch}(t) \le P_{ch}^{max}, \quad 0 \le \sum_{n=1}^{N} P_{n,dis}(t) \le P_{dis}^{max} \tag{40}$$

where $S(t)$ is the stored energy at time t; η_{ch} and η_{dis} are efficiencies; E_{bat}^{max} is the maximum capacity. Equation (39) ensures the sustainability of the storage cycle.

3.3.6. Network Transmission Constraints

To prevent line congestion and ensure system safety, the power flow through the connecting lines between MGOs and the Alliance must not exceed the line capacity:

$$|P_{n,sell}(t) - P_{n,buy}(t)| \le P_{line,n}^{max} \tag{41}$$

where $P_{line,n}^{max}$ represents the maximum transmission power limit of the tie-line connecting MGO n.

3.4. Solution Algorithm

The proposed co-optimized scheduling model is a typical bi-level optimization problem [35]. The upper-level model (Alliance) determines the energy prices and reputation scores, while the lower-level model (MGOs) optimizes their internal scheduling and trading strategies. This hierarchical interaction is solved using an iterative algorithm based on the Stackelberg game theory. The solution process is implemented in MATLAB R2025b combined with CPLEX 12.10. The specific steps are as follows:

1. **Initialization**: Set the initial iteration index $k = 1$, maximum iteration k_{max}, and convergence precision ϵ. Initialize the time-of-use prices and reputation scores.
2. **Lower-level Optimization**: MGOs receive price signals and solve Equation (13) to obtain optimal power output and trading plans ($P_{n,sell}$, $P_{n,buy}$).
3. **Upper-level Optimization**: The Alliance collects MGO strategies and updates prices and reputation scores to maximize Equations (10)–(12), considering network constraints.
4. **Convergence Check**: Calculate the deviation of prices and revenues between iterations. If deviation $< \epsilon$ or $k > k_{max}$, stop and output results; otherwise, update prices and let $k = k + 1$, return to Step 2.

4. Case Analysis

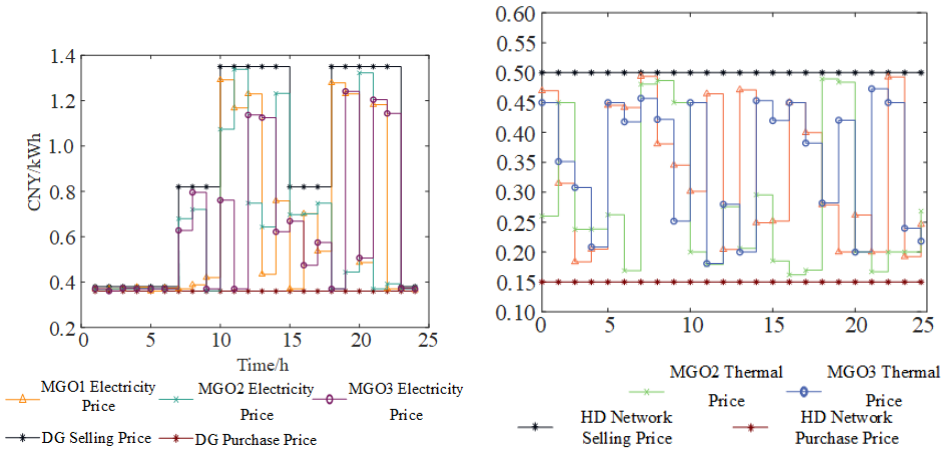
In order to verify the validity of the model proposed in this chapter, the MMG consisting of three MGOs is selected as the research object, using representative electrical/thermal load and renewable generation profiles for the three MGOs. Four scenarios are established to validate the effectiveness of the proposed mechanism:

- **Scenario 0 (Benchmark)**: A basic operation scenario without the reputation point trading mechanism, utilizing a fixed carbon price and fixed network tariffs. This serves as the baseline to purely evaluate the physical system performance.
- **Scenario 1**: A scenario considering demand response and the traditional fixed carbon transaction cost model, but without the dynamic reputation and network pricing mechanisms.
- **Scenario 2**: A scenario incorporating the reward and punishment step-type carbon transaction model but excluding the demand response capabilities.
- **Scenario 3 (Proposed)**: The comprehensive model proposed in this study, integrating the reputation point trading mechanism, step-type carbon trading, dynamic Shapley value-based network pricing, and demand response.

4.1. The Economic Analysis of the MMG

The revenues of each subject of the MMG under the three different operation scenarios are shown in Table 1. When compared with Scenario 1, the revenue of Alliance, MGO2, and MGO3 in Scenario 3 decreases slightly. However, the total revenue of the MMG is similar to that of Scenario 1 and even increases by 0.2% [29]. This indicates that the reward and punishment step-type carbon transaction cost model is comparable to the traditional model in enhancing system economics. In fact, it performs slightly better. In comparison with Scenario 2, after considering the demand response of the electric and thermal loads in Scenario 3, the revenue of all subjects increased. The revenues of the Alliance, MGO1, MGO2, MGO3, and SESO have increased by 33.00%, 16.00%, 4.08%, 5.95 and 20.00%, respectively [31]. This suggests that considering the demand response in the scheduling of the MMG system can effectively increase the revenue of each subject. In Scenario 3, the dynamic network tariff implemented via the Shapley value method ensures the stability of the Alliance's revenue ($\$47.61 \times 10^3$) relative to Scenario 1. Simultaneously, it effectively curbs "free-riding" behaviors through a fair cost allocation mechanism. This supports the

optimization of overall benefits. The time-of-use energy prices of each MGO are shown in Figure 3.



(**a**) (**b**)

Figure 3. Time-of-use energy pricing for Scenario 3 MGO. (**a**) Scenario 3 MGO time-of-use energy electricity price. (**b**) Scenario 3 MGO time-of-use energy heat price.

Table 1. Revenue of MMG system subjects under 3 scenarios (Unit: 10^3 USD).

Revenue Type	Scenario 1	Scenario 2	Scenario 3
Alliance Revenue	47.97	35.77	47.61
MGO1 Revenue	157.36	141.06	163.63
MGO2 Revenue	169.87	162.37	168.98
MGO3 Revenue	318.93	297.46	315.14
SESO Revenue	39.82	33.52	40.22
Total Revenue	733.95	670.18	735.41

Note: All values are converted from CNY to USD using an exchange rate of 6.9546.

4.2. Carbon Emission Analysis

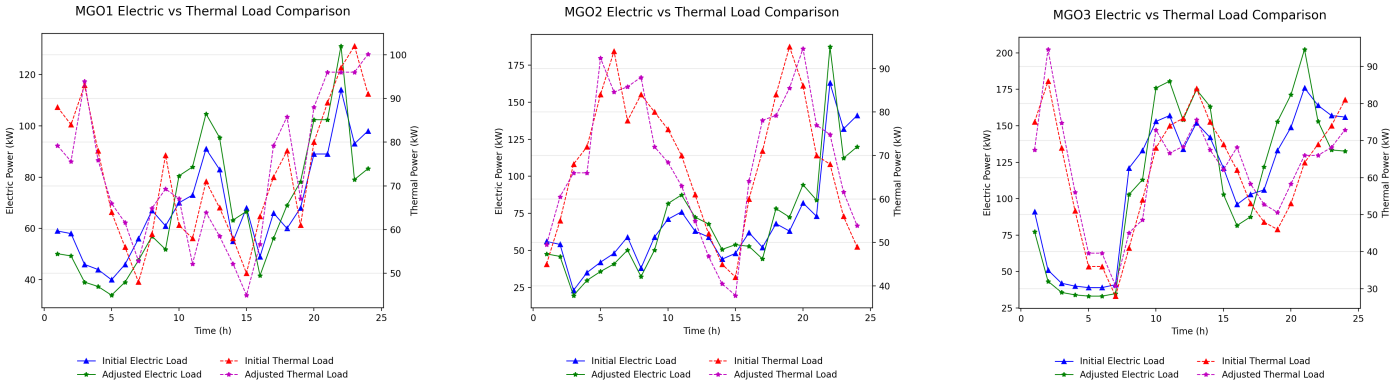
Comparative analysis revealed significant variations in carbon emissions and trading costs under different operational strategies. In Scenario 3, the adoption of a reward–penalty step-type carbon pricing mechanism reduces system emissions by 35 tons (from 3799.1 to 3764.1 tons) compared to Scenario 1, albeit with a \$2.83 $\times$ 10^3 increase in carbon trading cost (from \$17.27 $\times$ 10^3 to \$20.10 $\times$ 10^3) [10]. This divergence stems from the dynamic pricing structure of Scenario 3, in which emissions exceeding predefined thresholds trigger progressive cost increments, whereas Scenario 1 employs a fixed carbon price. Notably, despite the higher carbon costs, Scenario 3 achieves a marginally improved MMG revenue (Table 1), demonstrating the model's ability to balance economic and environmental objectives. Further optimization was observed when demand response was integrated (Scenarios 3 vs. 2). Load-shifting strategies reduced emissions by 49.6 tons (3813.4 tons to 3764.1 tons) and lowered carbon costs by \$8.45 $\times$ 10^3 (from \$28.55 $\times$ 10^3 to \$20.10 $\times$ 10^3). This improvement is attributed to the temporal redistribution of demand to periods with abundant renewable generation, minimizing reliance on carbon-intensive GTs and GBs.

4.3. Demand Response Analysis

During low renewable output periods (1:00–9:00 with WT low, PV starting after 7:00; 23:00–24:00 with PV off and low WT), MGO1 cuts the electric load, peaking at 14.70 MW (24:00). Curtailed loads shifted to high-output periods (10:00–15:00, 19:00–22:00), reaching 17.10 MW at 22:00. Figure 4a–c show that MGO2-3 exhibit similar responses: MGO2 curtails

21.15 MW (24:00) and peaks at 24.45 MW (22:00); MGO3 curtails 23.55 MW (23:00) and peaks at 26.4 MW (21:00).

Figure 4a shows that MGO1 reduces the thermal load during 9:00–15:00 due to the high renewables reducing the GT heat output. The shifted thermal load peaks at 9.10 MW (24:00). Figure 4b,c confirm the analogous MGO2-3 thermal responses: MGO2 peaks at 8.60 MW (20:00) and MGO3 at 8.60 MW (2:00).



(**a**) (**b**) (**c**)

Figure 4. Electric vs. thermal load comparison for MGO units. (**a**) MGO1 electric vs. thermal load comparison; (**b**) MGO2 electric vs. thermal load comparison; (**c**) MGO3 electric vs. thermal load comparison.

4.4. Analysis of the MMG Scheduling Result

Figure 5 presents the operational results of Scenario 3. MGO1-3 supply surplus electricity during high renewable output periods (9:00–15:00), reducing the GT output to zero and selling up to 80 MW to the Alliance [14]. During low renewable output, MGO1 primarily uses a GT and purchases from other MGOs (max 72.80 MW from MGO2 at 23:00). MGO2-3 requires SESO support during evening peaks, with discharges of 80.45 MW (22:00) and 94.4 MW (21:00), respectively [31].

During low renewable periods, MGO1-3 GTs operate at high output to meet electrical loads while generating significant heat [27]. The thermal demand is primarily covered by GTs, with limited inter-MGO thermal exchange owing to small load differences.

4.5. Dynamic Game Process and System Robustness Analysis

To validate the constraint effect of the proposed transaction mechanism on fraudulent and default behaviors, two scenarios were simulated under the framework of Scenario 3 [12]:Scenario 1 (baseline with no violations) and Scenario 2 (MGO3 commits data fraud on Day 2; MGO2 violates energy interaction agreements on Day 5). The results demonstrate that the reputation-point mechanism effectively regulates stakeholder revenue and transaction prioritization. It shows that the penalty factor γ effectively increases the cost of violation in the actual game. This prompts MGOs to shift towards honest trading strategies. On Day 1, all MGOs operated with compliance. MGO3 achieved the highest emission reduction target without any defaults, and thus earned a reward of 1 point, raising its reputation score from the initial 3 points to 4 points. However, on Day 2, MGO3 was prohibited from internal transactions because of a severe data fraud. According to the penalty rules, this severe violation incurred a 2-point penalty. This led to a significant increase in energy procurement costs and energy storage leasing fees. Simultaneously, its reliance on high-carbon GT/GB units raised pollutant penalty costs [18]. This resulted in a daily revenue decrease of $\$4.33 \times 10^3$ ($\$304.66 \times 10^3$ vs. $\$308.99 \times 10^3$) and a reduction in reputation points from 4 to 2. Starting on Day 3, MGO3 lost transaction priority owing

to low points and was subjected to penalty pricing for energy purchases [14], incurring revenue losses of \$1.02 × 10^3 and \$4.76 × 10^3 on Days 3–4, respectively. By proactively reducing carbon emissions, MGO3 restored its points to 6 by Day 7, achieving a revenue of \$338.62 × 10^3 (a 2.32% increase over Scenario 1). This confirms the incentive effect of point restoration on revenue recovery [15]. Following MGO2's default on Day 5, its reputation points decreased from 3 to 2. Consequently, daily revenue declined by 10.86% (\$181.34 × 10^3 vs. \$203.42 × 10^3). Subsequent revenue losses on Days 6–7 ranged between 6.5–9.8%. Despite compliance, MGO1 experienced revenue reductions of 6.72–16.44% on Days 5–7 due to lower point rankings [29]. This highlights the competitive edge of high-ranking MGOs in trading activities.

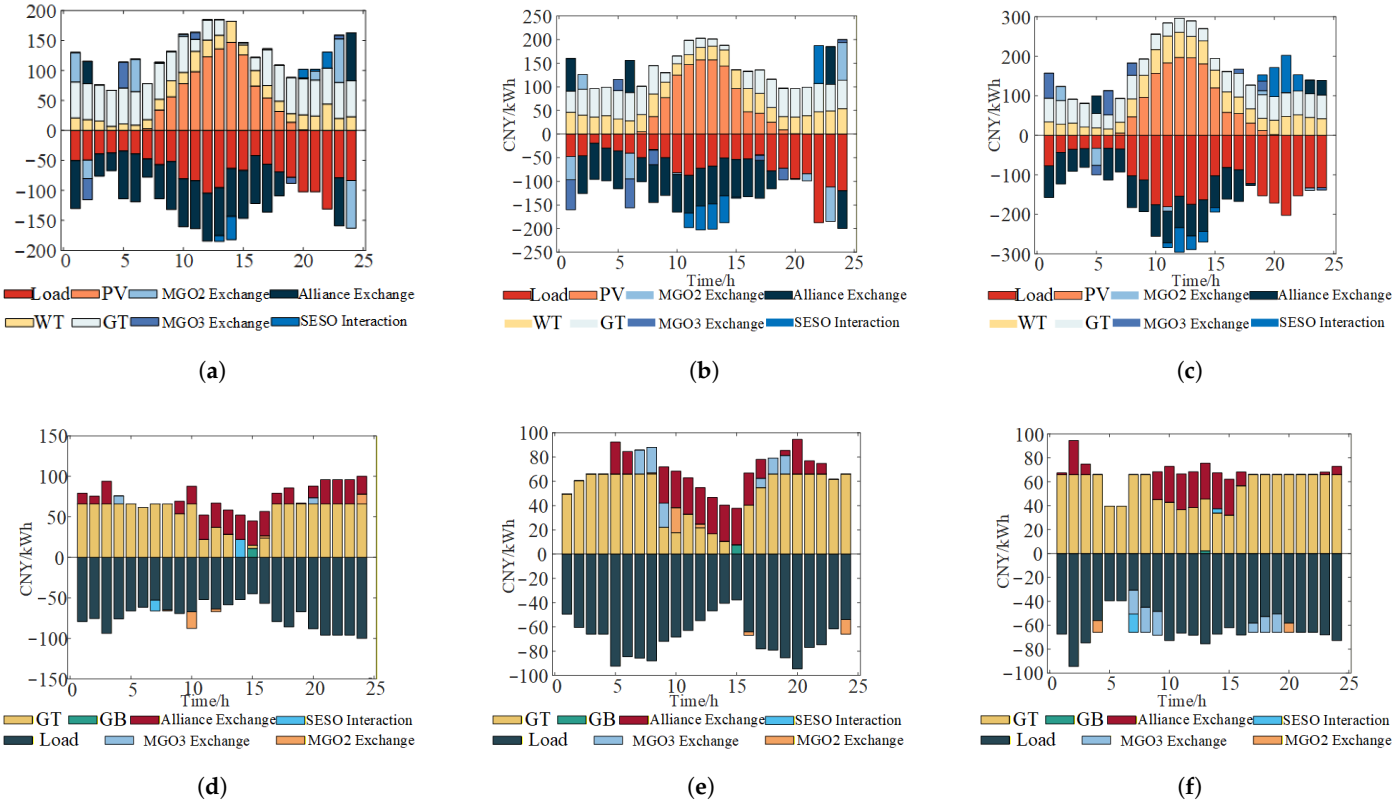


Figure 5. Power balance analysis for MGO units: Top row shows electric power balance; bottom row shows thermal power balance. (**a**) MGO1 electric power balance; (**b**) MGO2 electric power balance; (**c**) MGO3 electric power balance; (**d**) MGO1 thermal power balance; (**e**) MGO2 thermal power balance; (**f**) MGO3 thermal power balance.

4.6. Scalability Analysis

Although the current case study operates within a 3-MGO topology, the mathematical structure of the proposed mechanism ensures excellent scalability to broader urban network implementations. The problem is formulated entirely as a mixed-integer linear programming (MILP) model. For the current testbed, iterative convergence via real-world commercial solvers (e.g., CPLEX 12.10) takes practically insignificant computational efforts (in seconds). Scaling the model constraints dynamically from 10 to 50 interdependent microgrid operators entails only polynomial expansions, enabling global optimal outputs well within customary day-ahead and intra-day clearance timelines (a few minutes). By effectively coupling physical dispatch constraints inside market negotiations, this model demonstrates substantial applicability toward realistic large-scale Smart City developments.

5. Conclusions

Under the distributed transaction framework, an energy transaction mechanism based on reputation points is proposed to guarantee the revenue of each MMG subject. Additionally, a low-carbon economic scheduling model is established, incorporating demand response and a reward–punishment step-type carbon transaction model. Finally, the following conclusions were obtained through the case study:

1. In the scheduling model, compared with other carbon emission-related models, the reward and punishment step-type carbon transaction model can reduce the system carbon emission more effectively while keeping the revenue of the MMG system not reduced;
2. After considering demand response, by shifting part of the load to new energy output or peak energy supply hours, users avoid the increase in system carbon emission caused by increasing equipment output to meet load demand during energy shortage hours, which increases system revenue and reduces system carbon emission;
3. Compared with other scenarios, after considering the reward and punishment step-type carbon transaction model and demand response, the system revenue increases by 0.20% and 9.73% respectively, and the carbon emission decreases by 0.92% and 1.29% respectively, which fully verifies the economy and low-carbon nature of the proposed scheduling strategy;
4. Under the trading mechanism of reputation points, the changes in MGO revenue are related to the reputation points, which fully verifies that the mechanism proposed in this paper can effectively protect the revenue of subjects with good reputation and promote the subjects to fulfill the contract honestly and actively.

The results presented in this study carry direct implications for Smart City energy governance. Unlike blockchain-based governance schemes that require substantial computational overhead [2], the proposed reputation mechanism operates without distributed consensus protocols, offering a lightweight and practically deployable alternative for urban smart grid management. Furthermore, by integrating P2P energy trading with carbon emission regulation and dynamic network pricing, the framework aligns closely with the requirements of Smart City low-carbon transition strategies, as evidenced by recent advances in multi-microgrid scheduling under carbon trading environments [20] and P2P electricity–carbon coupled distribution networks [21]. These findings suggest that the proposed model is well-suited for deployment within the intelligent energy infrastructure of modern Smart Cities. The step-type carbon transaction cost model established in this study adopts a fixed carbon quota and fixed base price, which does not fully utilize the vitality of the carbon transaction market. Relevant optimization models can be established to optimize the carbon transaction parameters and realize parameter adaptation in the process of subsequent research. Furthermore, while the current model addresses electrical and thermal energy, the proposed "Social–Economic–Physical" framework can be seamlessly extended to multi-energy microgrids involving gas and cooling networks in future works, aligning with recent advances in comprehensive multi-energy coupling [36].

Author Contributions: Conceptualization, H.W. and D.Y.; methodology, H.W.; software, J.F.; validation, X.M., H.Z. and H.D.; formal analysis, H.W.; investigation, J.F.; resources, D.Y.; data curation, X.M.; writing—original draft preparation, H.W.; writing—review and editing, D.Y.; visualization, J.F.; supervision, D.Y.; project administration, H.D.; funding acquisition, D.Y. All authors have read and agreed to the published version of the manuscript.

Funding: This research received no external funding.

Data Availability Statement: Data is contained within the article.

Acknowledgments: The authors would like to thank the anonymous reviewers for their constructive comments. During the preparation of this manuscript, the authors used Gemini 3.1 for the purpose of English language polishing, and Claude Sonnet 4.6 for the purpose of assisting in writing partial auxiliary code. The authors have reviewed and edited the output rigorously and take full responsibility for the originality, validity, and integrity of the content of this publication.

Conflicts of Interest: Author Hui Deng was employed by the company Zhongxinjian Electric Power Group Co., Ltd. The remaining authors declare that the research was conducted in the absence of any commercial or financial relationships that could be construed as a potential conflict of interest.

Abbreviations

The following abbreviations are used in this manuscript:

MMG	Multi-Microgrid
MGO	Microgrid Operator
GT	Gas Turbine
GB	Gas Boiler
SESO	Shared Energy Storage Operator
RMSE	Root Mean Square Error
MAE	Mean Absolute Error
DTW	Dynamic Time Warping
MILP	Mixed-Integer Linear Programming

Nomenclature

Sets and Indices	
n, t	Index of microgrid operator (MGO) and time period
T	Total number of time periods in a scheduling cycle
Ω_{MGO}	Set of all detailed microgrid operators
Parameters	
$\lambda_s(t), \lambda_p(t)$	Buying and selling electricity prices of the higher-level energy network
$\lambda_{h,s}(t), \lambda_{h,p}(t)$	Buying and selling heat prices of the higher-level energy network
$P_{n,load}(t), P_{n,h,load}(t)$	Electrical and thermal load of MGO n
$P_{PV}(t), P_{WT}(t)$	Power output of Photovoltaic and Wind Turbine
$E_{n,0}(t)$	Initial carbon emission quota
γ	Penalty factor
γ_{bas}	Base penalty factor
τ	Penalty factor growth rate
ν	Step carbon price rise
ω	Carbon emission interval length
$\phi_j(t)$	Shapley value marginal contribution of MGO j
$P_{GT}^{max}, P_{GT}^{min}$	Maximum and minimum output limits of Gas Turbine
$Q_{GB}^{max}, Q_{GB}^{min}$	Maximum and minimum output limits of Gas Boiler
$R_{GT}^{up}, R_{GT}^{down}$	Ramp up and down limits for Gas Turbine
$R_{GB}^{up}, R_{GB}^{down}$	Ramp up and down limits for Gas Boiler
$E_{bat}^{max}, E_{bat}^{min}$	Maximum and minimum capacity of shared energy storage
η_{ch}, η_{dis}	Charging and discharging efficiency of storage
P_{line}^{max}	Maximum transmission capacity of tie-lines
Variables	
$P_{n,sell}(t), P_{n,buy}(t)$	Power sold/purchased by MGO n to/from Alliance
$P_{n,GT}(t), Q_{n,GB}(t)$	Output power of Gas Turbine and Gas Boiler
$P_{n,ch}(t), P_{n,dis}(t)$	Charging and discharging power of MGO n
$S(t)$	State of Charge (SOC) of the energy storage system
μ_n	Reputation state binary variable (1=normal, 0=fraud/default)

References

1. Hassine, L.; Quadar, N.; Ledmaoui, Y.; Chaibi, H.; Saadane, R.; Chehri, A.; Jakimi, A. Enhancing smart grid security in smart cities: A review of traditional approaches and emerging technologies. *Appl. Energy* **2025**, *398*, 126430. [CrossRef]
2. Xu, Z.; Shahraki, A.S.; Rudolph, C. Blockchain-based malicious behaviour management scheme for smart grids. *Smart Cities* **2023**, *6*, 3005–3031. [CrossRef]
3. Silva, N.S.E.; Castro, R.; Ferrão, P. Smart grids in the context of smart cities: A literature review and gap analysis. *Energies* **2025**, *18*, 1186. [CrossRef]
4. Tushar, W.; Saha, T.K.; Yuen, C.; Liddell, P.; Bean, R.; Poor, H.V. Peer-to-peer energy trading with sustainable user participation: A game theoretic approach. *IEEE Access* **2018**, *6*, 62932–62943. [CrossRef]
5. Wang, Z.; Chen, B.; Wang, J.; Begovic, M.M.; Chen, C. Coordinated energy management of networked microgrids in distribution systems. *IEEE Trans. Smart Grid* **2014**, *6*, 45–53. [CrossRef]
6. Ferrag, M.A.; Maglaras, L. DeepCoin: A novel deep learning and blockchain-based energy exchange framework for smart grids. *IEEE Trans. Eng. Manag.* **2020**, *67*, 1285–1297. [CrossRef]
7. Wu, J.; Zhao, P.; Li, L.; Shi, F.; Li, B. Multi-microgrids distributed peer-to-peer energy trading in distribution system considering uncertainty risk. *Int. J. Electr. Power Energy Syst.* **2023**, *152*, 109234. [CrossRef]
8. Guerrero, J.; Chapman, A.C.; Verbič, G. Decentralized p2p energy trading under network constraints in a low-voltage network. *IEEE Trans. Smart Grid* **2018**, *10*, 5163–5173. [CrossRef]
9. Zhang, S.; Zheng, K.; Wang, B. A v2v electricity transaction scheme with privacy protection based on the internet of vehicles and consortium blockchain. *Int. J. Electr. Power Energy Syst.* **2024**, *157*, 109789. [CrossRef]
10. Janko, S.; Johnson, N.G. Reputation-based competitive pricing negotiation and power trading for grid-connected microgrid networks. *Appl. Energy* **2020**, *277*, 115598. [CrossRef]
11. Sun, C.; Liu, Y.; Li, Y.; Lin, S.; Gooi, H.B.; Zhu, J. Network-aware p2p multi-energy trading in decentralized electric-heat systems. *Appl. Energy* **2023**, *345*, 121298. [CrossRef]
12. Shi, Q.; Hao, Y.; Ren, H.; Huang, X. Blockchain-based distributed electricity transaction model. *Int. J. Energy Res.* **2022**, *46*, 11278–11290. [CrossRef]
13. Zhang, X.; Wang, Z.; Lu, Z. Multi-objective load dispatch for microgrid with electric vehicles using modified gravitational search and particle swarm optimization algorithm. *Appl. Energy* **2022**, *306*, 118018. [CrossRef]
14. Paudel, A.; Sampath, L.P.M.I.; Yang, J.; Gooi, H.B. Peer-to-peer energy trading in smart grid considering power losses and network fees. *IEEE Trans. Smart Grid* **2020**, *11*, 4727–4737. [CrossRef]
15. Yin, S.; Ai, Q.; Li, J.; Li, D.; Guo, Q. Trading mode design for a virtual power plant based on main-side consortium blockchains. *Appl. Energy* **2022**, *325*, 119932. [CrossRef]
16. Cui, Y.; Xu, Y.; Huang, T.; Wang, Y.; Cheng, D.; Zhao, Y. Low-carbon economic dispatch of integrated energy systems that incorporate ccpp-p2g and pdr considering dynamic carbon trading price. *J. Clean. Prod.* **2023**, *423*, 138812. [CrossRef]
17. Wang, S.; Wang, S.; Zhao, Q.; Dong, S.; Li, H. Optimal dispatch of integrated energy station considering carbon capture and hydrogen demand. *Energy* **2023**, *269*, 126981. [CrossRef]
18. Zheng, W.; Xu, Z.; Shao, Z.; Li, J.; Lei, K.; Li, J. Optimal dispatch of nearly-zero carbon integrated energy system considering waste incineration plant-carbon capture system and market mechanisms. *Int. J. Hydrogen Energy* **2023**, *48*, 27013–27031. [CrossRef]
19. Elkholy, M.H.; Senjyu, T.; Elymany, M.; Gamil, M.M.; Talaat, M.; Masrur, H.; Ueda, S.; Lotfy, M.E. Optimal resilient operation and sustainable power management within an autonomous residential microgrid using african vultures optimization algorithm. *Renew. Energy* **2024**, *224*, 120247. [CrossRef]
20. Thampanichvong, K.; Ongsakul, W.; Singh, J.G. Multi-microgrids optimal scheduling incorporating CO_2 and peer-to-peer energy trading considering demand response and electric vehicle loads using adaptive robust optimisation. *IET Smart Grid* **2025**, *8*, e70045. [CrossRef]
21. Ma, H.; Xiang, Y.; Zhao, A.P.; Li, S.; Liu, J. Optimal peer-to-peer coupled electricity and carbon trading in distribution networks. *Engineering* **2025**, *51*, 37–48. [CrossRef]
22. Zhu, G.; Wu, J.; Li, K.; Tan, S.C.; Hui, S.Y.R. Frequency-Splitting-Free Wireless Power Transfer via Hybrid Frequency Control and Asymmetric Voltage Cancellation. *IEEE Trans. Ind. Electron.* **2026**, 1–14. [CrossRef]
23. Karimi, H. Optimal operation scheduling of water-energy nexus multi-microgrid systems integrated with energy storage systems and renewable energy. *Energy* **2026**, *345*, 140221. [CrossRef]
24. Zhang, R.; Li, X.; Fu, L.; Jiang, T.; Li, G.; Chen, H. Network-aware energy management for microgrids in distribution market: A leader-followers approach. *Appl. Energy* **2023**, *332*, 120522. [CrossRef]
25. Ullah, M.H.; Park, J.D. Peer-to-peer energy trading in transactive markets considering physical network constraints. *IEEE Trans. Smart Grid* **2021**, *12*, 3390–3403. [CrossRef]
26. Liu, X.; Chen, X.; Jin, T.; Liu, Z.; Liu, Y.; Su, M.; Li, C.; Wu, Q. Network-constrained peer-to-peer energy trading for multiple microgrids considering zoning pricing. *Int. J. Electr. Power Energy Syst.* **2023**, *147*, 108837. [CrossRef]

27. Dong, H.; Fu, Y.; Jia, Q.; Wen, X. Optimal dispatch of integrated energy microgrid considering hybrid structured electric-thermal energy storage. *Renew. Energy* **2022**, *199*, 628–639. [CrossRef]
28. Wang, J.; Yang, Y. Research on the resilience of reputation mechanism to the cooperative environment in the face of external shocks. *Appl. Math. Comput.* **2026**, *510*, 129713. [CrossRef]
29. Seyednouri, S.R.; Safari, A.; Farrokhifar, M.; Ravadanegh, S.N.; Quteishat, A.; Younis, M. Optimal stochastic scheduling of a multi-carrier multi-microgrid system considering storages, demand responses, and thermal comfort. *Sustain. Cities Soc.* **2023**, *99*, 104943. [CrossRef]
30. Li, Y.; Zhou, Y.; Wang, J.; Ding, J.; Wei, C.; Liu, Z. Co-optimization of configuration and energy scheduling of multi-communities microgrid systems considering carbon-green certificate trading mechanism. *Energy* **2026**, *344*, 139864. [CrossRef]
31. Alzahrani, A.; Sajjad, K.; Hafeez, G.; Murawwat, S.; Khan, S.; Khan, F.A. Real-time energy optimization and scheduling of buildings integrated with renewable microgrid. *Appl. Energy* **2023**, *335*, 120640. [CrossRef]
32. Yan, N.; Ma, G.; Li, X.; Guerrero, J.M. Low-carbon economic dispatch method for integrated energy system considering seasonal carbon flow dynamic balance. *IEEE Trans. Sustain. Energy* **2023**, *14*, 576–586. [CrossRef]
33. Wang, Y.; Tan, Z.; Zhou, X.; Li, J.; Hu, Y.; Wu, H.; Ju, L. A coordinated operation optimization model for multiple microgrids and shared energy storage based on asymmetric bargaining negotiations. *Processes* **2025**, *13*, 2514. [CrossRef]
34. Zhu, Y.; Gu, W.; Li, Q.; Meng, Y.; Zhang, K.; Liu, P. Co-optimized operation of multi-integrated energy microgrids-shared energy storage plants based on mixed game theory. In *Proceedings of the 2025 4th International Conference on New Energy System and Power Engineering (NESP)*; IEEE: Piscataway, NJ, USA, 2025; pp. 518–524.
35. Cheng, Y.; Zou, H.; Wang, F. Low-carbon and economic-oriented dispatch method for multi-microgrid considering green certificate: Carbon trading mechanism driven by AI reinforcement learning-enhanced genetic algorithm. *Processes* **2025**, *13*, 2531. [CrossRef]
36. Multi-energy coupling units scheduling and management. *IEEE Trans. Smart Grid* **2025**, *16*, 2144–2155. [CrossRef]

Disclaimer/Publisher's Note: The statements, opinions and data contained in all publications are solely those of the individual author(s) and contributor(s) and not of MDPI and/or the editor(s). MDPI and/or the editor(s) disclaim responsibility for any injury to people or property resulting from any ideas, methods, instructions or products referred to in the content.